Materials Science-Poland, *Vol. 27*, *No. 1*, *2009*

Characterization of polypyrrole films deposited on aluminum surfaces from oxalic acid aqueous solution

A. S. LIU*, M. A. S. OLIVEIRA

Departamento de Química, Instituto Tecnológico de Aeronáutica (ITA),
Pça Mal Eduardo Gomes, 50 – CTA, São José dos Campos, SP, Brasil, CEP 12228-900

Electrochemical synthesis of polypyrrole films (PPy) on aluminum surfaces from oxalic acid aqueous solutions was performed using the cyclic voltammetry and galvanostatic technique. SEM micrographs of aluminum surfaces coated with PPy films showed that the galvanostatically deposited films were more homogeneous than those deposited by cyclic voltammetry. The presence of bands at 1170 and 1630 cm^{-1} in the FTIR spectra of the PPy films indicate that the films are overoxidised. The corrosion protection of aluminum surfaces coated with polypyrrole films was investigated by potentiodynamic polarization curves and electrochemical impedance spectroscopy in a chloride medium. A poor corrosion protection performance of the PPy films was observed and it was associated with the overoxidation process, resulting in defects and pores along the polymeric chain that allows penetration of corrosive species.

Key words: *polypyrrole; aluminum; oxalic acid; overoxidation*

1. Introduction

Polypyrrole (PPy) is a material extensively investigated because of its high conductivity, environmental stability, wide range of applications such as membranes, sensors, batteries, anti-corrosion films, etc. [1–4]. Polymeric films can be synthesized from aqueous or organic media by chemical and electrochemical methods. Electrochemical synthesis is more advantageous, since the coating properties (thickness, conductivity and adherence) can be controlled by varying parameters such as current density, monomer concentration, electrolyte solution nature and pH [5–8].

Various research groups reported the electrodeposition of PPy on aluminum surfaces in various electrolytes such as sulfuric acid, sulphonates, sulfosuccinate, saccharin and nitric acid [9–13]. The formation of an Al/Al_2O_3 /PPy sandwich structure during the PPy electrodeposition has been suggested. Since the PPy films are deposited onto aluminum oxide, the nature of this layer (porous or compact) influences the electrodeposition process [10, 14, 15]. This mechanism suggests that pores and defects on

*Corresponding author, e-mail: dora@ita.br

aluminum oxide should act as active growth sites of the PPy film, and therefore a compact layer should hinder charge transfer reactions, inhibiting the monomer oxidation and consequently the PPy growth.

In the previous work, the authors showed that the formation of adherent and homogeneous PPy films on aluminum surfaces from aqueous solutions containing pyrrole and tartrate depends on the synthesis parameters such as the pH, monomer concentration, and the current density [16]. Even though oxalic acid medium has been studied for depositing polypyrrole on aluminum substrates [17–20], the corrosion protection of aluminum surfaces coated with PPy films have been little investigated.

In this work the influence of the conditions of synthesis on the properties of the PPy films deposited on 99.89 % wt. aluminum from aqueous solution containing oxalic acid was investigated. Additionally, the corrosion behaviour of aluminum surfaces coated with PPy films was investigated by potentiodynamic polarization and electrochemical impedance spectroscopy.

2. Experimental

Pyrrole (Merck) was distilled prior to use, and the electrolytes, oxalic acid (Baker) and sodium chloride (Reagen) were used as received. The electrochemical experiments were performed at room temperature in a one-compartment cell containing three electrodes. The working electrode was 99.89 wt. % aluminum, inlaid on Teflon®, with a disc shape exposed area of 0.53 cm^2. The reference electrode was a saturated Ag|AgCl, Cl^- electrode and the auxiliary electrode was a platinum wire. The solutions of electrolytes were prepared by dissolving 0.2 $mol \cdot dm^{-3}$ oxalic acid and 0.5 $mol \cdot dm^{-3}$ pyrrole in distilled water (pH = 0.8). The aluminum surfaces were polished with abrasive paper (220, 400, 600 and 1200 grits) and rinsed with distilled water before each electrochemical experiment. The PPy electrodeposition was carried out by cyclic voltammetry by scanning the potential between –1.0 and 2.0 V vs. Ag/AgCl at a sweep rate of 5.0 $mV \cdot s^{-1}$. The PPy film growth was also performed using the galvanostatic technique, namely by applying current densities ranging between 1.0 and 10.0 $mA \cdot cm^{-2}$ to the working electrode. The morphology of aluminum surfaces polished and coated with PPy films was analyzed using a Jeol JXA-840A scanning electron microscope (SEM). The micrographs were obtained using an electron beam of 15 keV.

FTIR was used to analyze the composition of the PPy films. The spectra were obtained using a spectrometer model Spectrum-2000 (Perkin Elmer) in the range of 4000–400 cm^{-1}, with 4 cm^{-1} resolution, 40 scans, at 25 ^oC. KBr pellets were prepared with solid oxalic acid and with the PPy films removed from aluminum surfaces. The corrosion resistance of aluminum surfaces, polished and coated with PPy films, was investigated using the potentiodynamic polarization technique and electrochemical impedance spectroscopy. The surfaces were exposed to unstirred 0.1 $mol \cdot dm^{-3}$ NaCl aqueous solution (pH = 5.9) open to the atmosphere.

The polarization curves were obtained starting from the open circuit potential (OCP) and varying the potential up to 400 mV in one set of experiments (anodic branch of the Tafel plot) and varying it down to –400 mV in another set of experiments (cathodic branch of the Tafel plot). The potential scan rate was 5 $mV \cdot s^{-1}$. The corrosion potential E_{corr} and the corrosion current densitiy j_{corr} were obtained from the Tafel plots. The E_{corr} is the potential at which the current density is zero. The j_{corr} was extrapolated from linear parts of the anodic and cathodic branches of the Tafel plots [21].

The impedance spectra were obtained over the frequency range 100 kHz–10 mHz, with acquisition of 10 points per decade, at an open circuit potential with AC excitation of 10 mV. A potentiostat/galvanostat model PGSTAT30 from Autolab, controlled by an USB-IF030 interface and by the FRA.EXE software both installed in a PC computer, was used to perform these experiments. The EQUIVCRT software developed by the Boukamp group [22] was used to determine the parameters related to the electrical equivalent circuits utilized to describe the electrochemical process occurring on each surface exposed to the aqueous solution containing chloride.

3. Results and discussion

3.1. Electrodeposition of PPy films by cyclic voltammetry

Figure 1 shows the results of the first cycle for the cyclic voltammetry experiments performed in the electrodeposition investigation of PPy from 0.2 $mol \cdot dm^{-3}$ oxalic acid solutions (pH 0.8) and varying the pyrrole concentration between 0.1 and 0.8 $mol \cdot dm^{-3}$. The curves were obtained by varying the potential from -1.0 to 2.0 V and back to -1.0 V at a sweep rate of 5 $mV\ s^{-1}$.

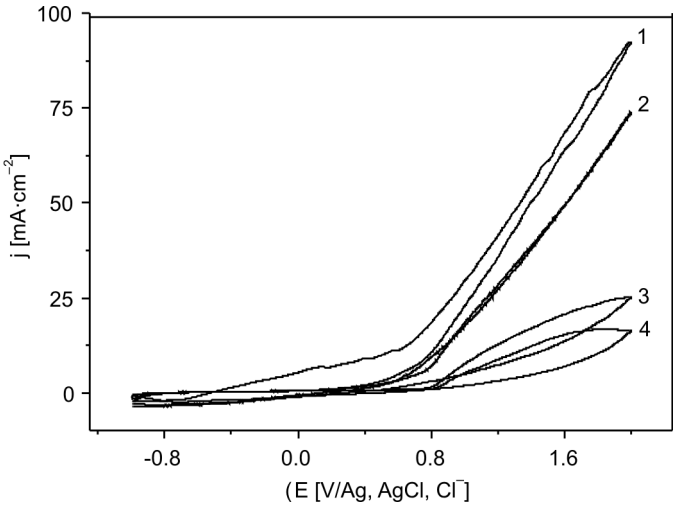

Fig. 1. Voltammetric profiles (first cycle) of PPy growth in 0.2 $mol \cdot dm^{-3}$ oxalic acid medium and pyrrole concentrations of: 1 – 0.8, 2 – 0.5, 3 – 0.2 and 4 – 0.1 $mol \cdot dm^{-3}$; sweep rate 5 $mV \cdot s^{-1}$

When the monomer concentration was 0.1 mol·dm^{-3}, the aluminum surface was not completely covered by the polymer. At 0.2 mol·dm^{-3} pyrrole, a homogeneous PPy film was electrodeposited on aluminum. The results in Fig. 1 also show that the potential at which the electropolymerization commences to decrease slightly with increasing monomer concentration. This behaviour may be associated with the diffusion process of pyrrole on the electrode surface which increases with the monomer concentration [5]. The higher the monomer concentration is, the faster the oxidation reaction of pyrrole at the interface aluminum/electrolyte solution, and the lower the potential at which the electropolymerization starts.

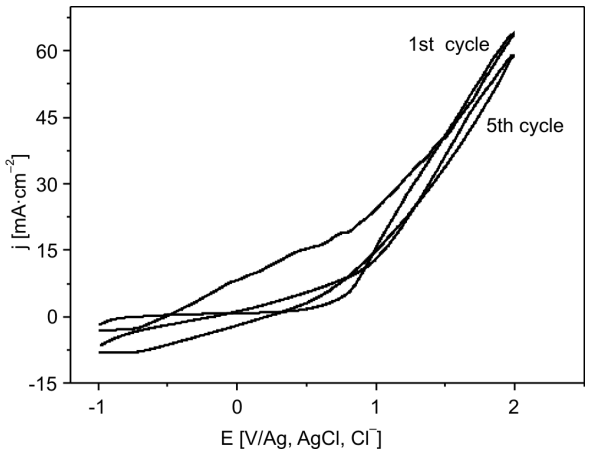

Fig. 2. Successive potentiodynamic growth of polypyrrole on aluminum electrode from aqueous solution containing 0.2 mol·dm^{-3} oxalic acid + 0.5 mol·dm^{-3} pyrrole, pH = 0.8 at the scan rate of 20 mV·s^{-1}

Figure 2 shows the cyclic voltammograms for the first and fifth cycles. The sweep rate of 20 mV·s^{-1} was used in this experiment. The current densities associated with the PPy growth decrease with the number of cycles. This behaviour differs from that reported in the literature for the growth of PPy coatings on AA2024 alloy from oxalic acid, where an increase of the current density was observed with the increase of number of cycles [19]. The behaviour observed in this work was ascribed to the overoxidation process resulting in an increase in the resistance of the coating due to a structural changes of the polymeric chains. This is an irreversible process that results in the shortening of the polymer chain length and/or formation of defects and pores along the PPy chain [23].

3.2. Galvanostatic deposition of polypyrrole films

PPy films were also deposited on aluminum surfaces by chronopotentiometry. Figure 3 shows some time dependences of potential obtained for PPy deposition from

aqueous solutions containing 0.2 mol·dm^{-3} oxalic acid and 0.5 mol·dm^{-3}pyrrole, pH = 0.8 and varying the current densities between 1.0 and 10.0 mA·cm^{-2}.

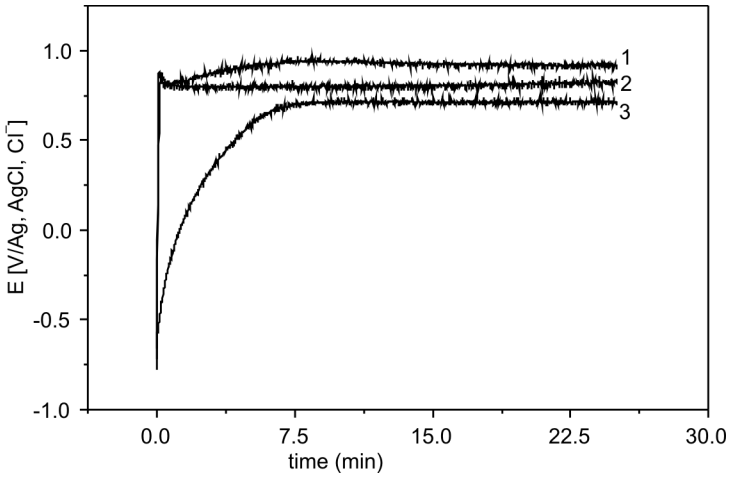

Fig. 3. Time dependences of potential curves for PPy electrodeposition from 0.2 mol·dm^{-3} oxalic acid + 0.5 mol·dm^{-3} pyrrole. The applied current densities (mA·cm^{-2}): 1 – 10; 2 – 5; 3 – 2.5 and 4 – 1.0

At the current density of 1.0 mA·cm^{-2}, the PPy film does not uniformly cover the entire aluminum surface. At 2.5 mA·cm^{-2}, the PPy film is homogeneous and the potential stabilizes at 0.8 V vs. Ag/AgCl and remains constant even after about 2 h after switching on the current. This result is in accordance with that observed in cyclic voltammetry, which showed that the PPy growth commences at 0.79 V vs. Ag/AgCl (curve 2 in Fig. 1). Films easily peeled off from the aluminum surfaces when the current densities higher than 2.5 mA·cm^{-2} were applied. This phenomenon has been observed for PPy films galvanostatically formed using high current densities, and might be associated with the occurrence of side reactions, induced by the high current density, which may result in short chain length or lead to formation of defects along the polymer chain [5]. Increasing the current densities results in a shift of the working potential to more positive values and in an increase of the thickness of the PPy films accompanied by a decrease in their adherence.

3.3. Morphology of PPy films, SEM micrographs

The morphology of aluminum surfaces coated with PPy films was investigated by SEM. The polymeric films were deposited on aluminum electrodes from 0.2 mol·dm^{-3} oxalic acid + 0.5 mol·dm^{-3} pyrrole aqueous solutions (pH = 0.8) by cyclic voltammetry (first cycle) at a sweep rate of 5 mV·s^{-1} and galvanostatically at 2.5 and 10 mA·cm^{-2} using the same deposition charge: 9.10^4 C·m^{-2}. Figure 4 shows these micrographs.

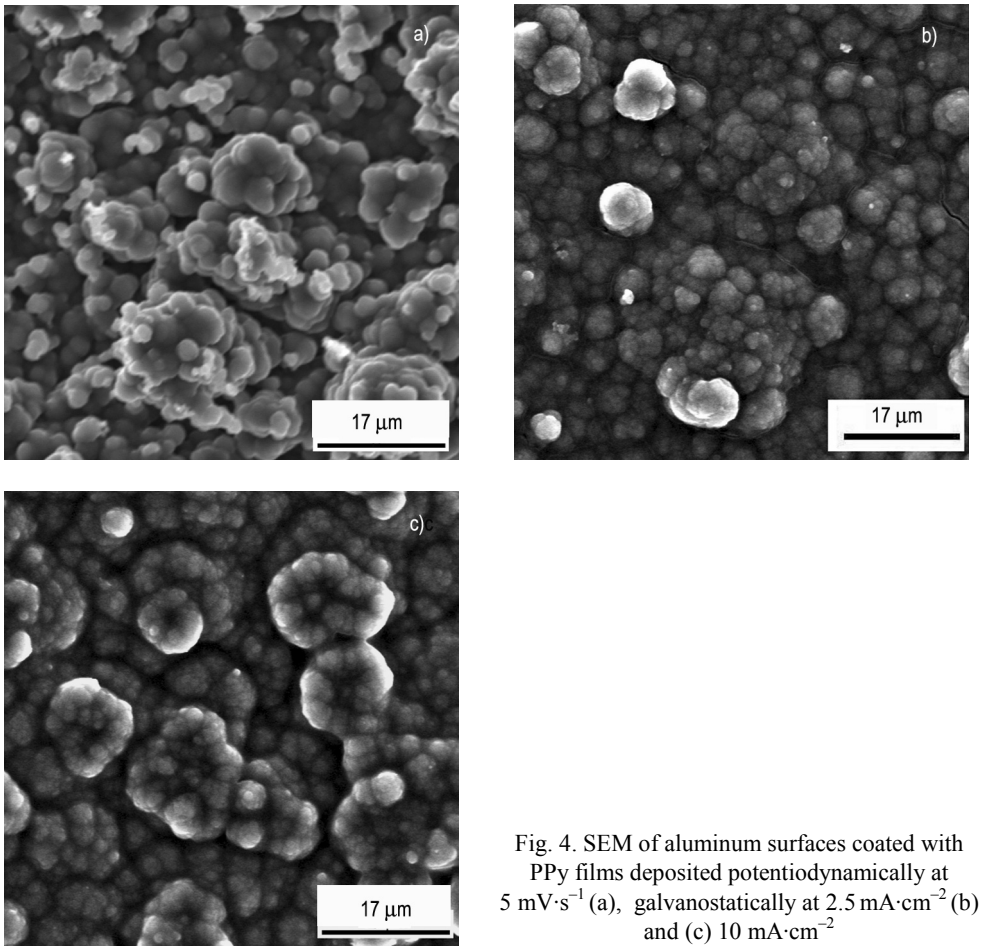

Fig. 4. SEM of aluminum surfaces coated with PPy films deposited potentiodynamically at 5 $mV \cdot s^{-1}$ (a), galvanostatically at 2.5 $mA \cdot cm^{-2}$ (b) and (c) 10 $mA \cdot cm^{-2}$

PPy films formed by cyclic voltammetry are less uniform than those deposited galvanostatically. The latter films are more homogeneous and present a cauliflower-like structure consisting of micro-spherical grains. It has been reported that this cauliflower structure is related to a difficult dopant intercalation in the disordered polymeric chain [24]. PPy films formed at higher current densities (10 $mA \cdot cm^{-2}$) exhibited smaller sized cauliflower-structures, with larger voids between them compared to the films formed at 2.5 $mA \cdot cm^{-2}$. The morphological differences between the films can be explained by side reactions which result in a short chain length, and/or lead to the formation of defects along the polymeric chain.

3.4. Fourier transform infrared (FTIR) spectra

FTIR analyses were used to investigate the composition of the PPy films removed from the aluminum surfaces. Figure 5 shows the FTIR spectra for oxalic acid (curve a)

and for the films formed. The PPy films were formed from 0.2 mol·dm^{-3} oxalic acid + 0.5 mol·dm^{-3} pyrrole containing aqueous solutions, pH = 0.8, by cyclic voltammetry (curve b), by varying the potential from –1.0 to 2.0 V and back to –1.0 V at the sweep rate of 5 mV·s^{-1} and galvanostatically, using the same amount of charge and current densities of 2.5 (curve c) and 10 mA·cm^{-2} (curve d).

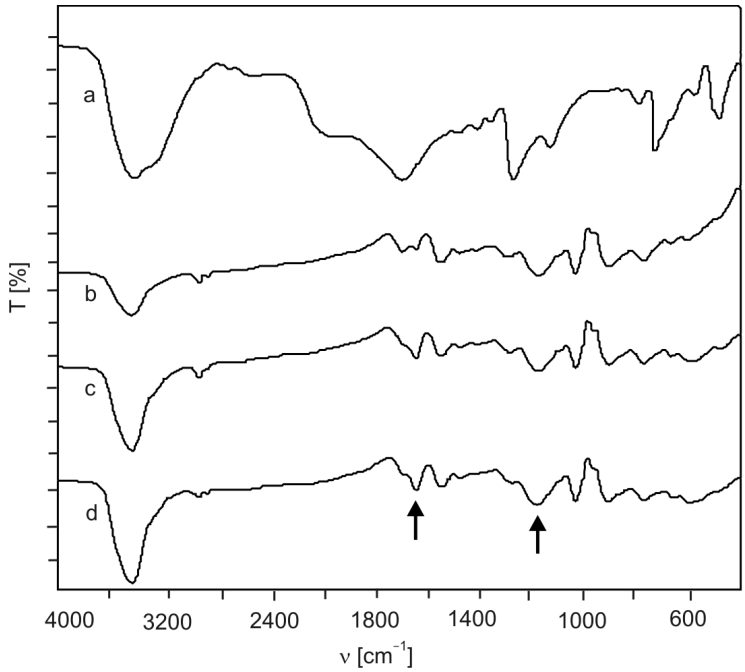

Fig. 5. FTIR spectra of: oxalic acid (a) and PPy films electrodeposited from aqueous solutions containing 0.2 mol·dm^{-3} oxalic acid + 0.5 mol·dm^{-3} pyrrole by cyclic voltammetry at 5 mV·s^{-1}(b), galvanostatically at 2.5 (c) and 10 mA·cm^{-2}(d)

The absorption bands at 1170 and 1630 cm^{-1} in the FTIR spectra of PPy films (marked with arrows in Fig. 5) have been attributed to the bipolaronic species and carbonyl groups that are formed in the overoxidation process of the PPy [25, 26].

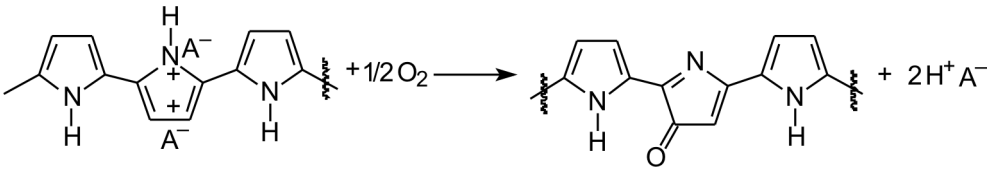

The intense absorption band of the carboxyl group of oxalic acid (at 1700 cm^{-1}) was not observed in the PPy films FTIR spectra. As suggested in the above reaction, overoxidised PPy should not contain significant amounts of oxalic acid.

These results differ from those for PPy films deposited at 2.5 mA·cm^{-2} in tartaric acid-containing medium. For films formed from solutions containing tartaric acid, an

intense band was observed at 1700 cm^{-1} in the FTIR spectrum, indicating that the tartaric acid had been incorporated into the film, and the bands at 1170 and 1630 cm^{-1} have not been observed in the FTIR spectra of the films [16]. This behaviour suggests that the PPy films formed in oxalic acid are more susceptible to the overoxidation process than those formed in tartaric acid.

The results presented in this work also differ from those reported in the literature for PPy films deposited on mild steel from an oxalic acid medium where the presence of an intense band at 1730 cm^{-1} in the FTIR spectrum was attributed to the doping process [27].

3.5. Corrosion tests

Figure 6 presents the potentiodynamic polarization curves obtained in 0.1 $mol \cdot dm^{-3}$ NaCl aqueous solutions (pH = 5.9) for uncoated aluminum surfaces and for those coated with PPy films galvanostatically electrodeposited at 2.5 and 10.0 $mA \cdot cm^{-2}$ from aqueous solutions containing pyrrole and oxalic acid, pH = 0.8.

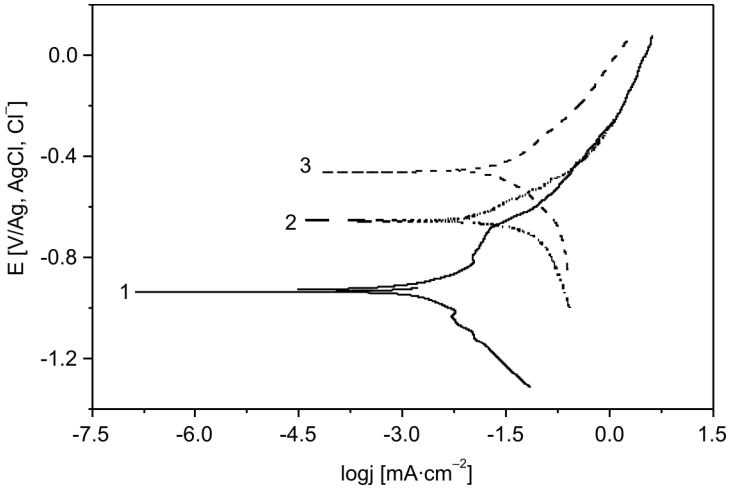

Fig. 6. Polarization curves at 5 $mV \cdot s^{-1}$ in aqueous solution 0.1 $mol \cdot dm^{-3}$ NaCl (pH = 5.9) for polished aluminum surface: 1 – uncoated; and coated with PPy films galvanostatically deposited at: 2 – 10 $mA \cdot cm^{-2}$ and 3 – 2.5 $mA \cdot cm^{-2}$

Table 1 shows the electrochemical parameters obtained from the polarization curves presented in Fig. 6. The corrosion current densities (j_{corr}) of the aluminum surfaces coated with PPy films were higher than those observed for uncoated aluminum surfaces. These results suggest that the PPy films formed in oxalic acid do not protect aluminum surfaces against corrosion.

The PPy coating does not act as a barrier; it does not prevent oxygen and chloride diffusion due to the permeability of the coating. Furthermore, the incorporation of the

chloride ions into the polymer could cause depassivation of the substrate and consequently the corrosion attack.

Table 1. Electrochemical parameters obtained by potentiodynamic polarization curves in NaCl solutions

Aluminum surfaces	Time to reach the OCP in the chloride medium [h]	E_{corr} [V/Ag, AgCl, Cl^-]	j_{corr} [mA·cm^{-2}]
Uncoated	48	–0.93	0.0023
Coated with PPy films deposited at pH = 0.8 and j = 10 mA·cm^{-2}	24	–0.67	0.019
Coated with PPy films deposited at pH = 0.8 and j = 2.5 mA·cm^{-2}	24	–0.46	0.024

Figure 6 shows that the cathodic current densities were higher for the aluminum surfaces coated with PPy than for the uncoated ones. Similar results have been reported in the literature; they have been associated with the reduction of the polymeric matrix, which contributes to an increase in the cathodic currents [28, 29]. A higher overoxidation degree of the PPy films formed at 10.0 mA·cm^{-2} would explain the lower cathodic current densities observed for that surface.

Electrochemical impedance spectroscopy (EIS) was also used to analyze the corrosion of the aluminum surfaces coated with PPy films. Figure 7 presents the Bode plots obtained for aluminum surfaces just polished and coated with PPy film deposited galvanostatically at 2.5 and 10.0 mA·cm^{-2} (maintaining the same deposition charge in 0.1 M NaCl aqueous solution, pH = 5.9).

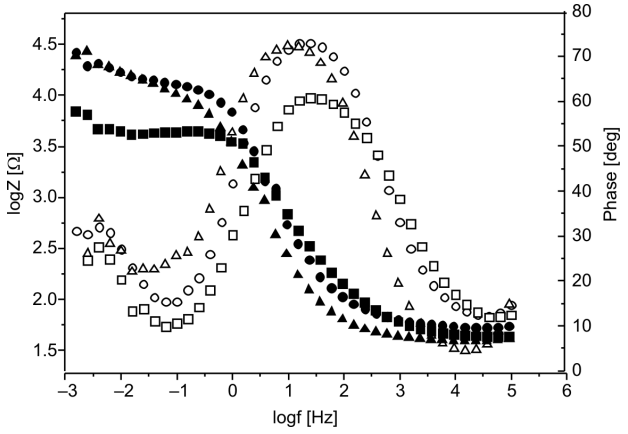

Fig. 7. Bode plot of: aluminum surfaces uncoated (triangles) and coated with PPy films deposited galvanostatically at 2.5 (circles) and 10.0 mA·cm^{-2} (boxes)

In the Bode plot, the ohmic resistance of the electrolytic solution is represented by a high-frequency plateau, while the low-frequency region can give information about the charge transfer resistance (R_{tc}) and film resistance (R_f). The impedance of uncoated

aluminum surfaces is similar to that of surfaces coated with PPy film deposited at 2.5 mA·cm^{-2}. This result confirms the poor performance of PPy film in protecting the aluminum surface against corrosion and it is in accordance with the polarization results presented in Fig. 6. Furthermore, it was observed that the impedance values for the aluminum surfaces coated with PPy film deposited at 2.5 mA·cm^{-2} are higher than those observed for the surfaces coated with film deposited at 10.0 mA·cm^{-2}. This result demonstrates the worst corrosion protection afforded by PPy of the films galvanostatically deposited from oxalic acid containing aqueous solutions at higher current densities (10 mA·cm$^{-2)}$.

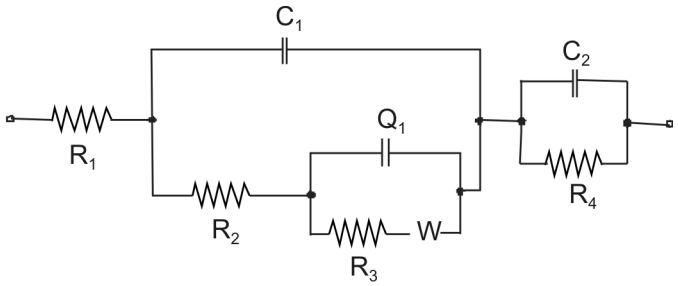

Fig. 8. Equivalent electric circuit model proposed to simulate the electrochemical behaviour of uncoated aluminum surface exposed to chloride medium (see the text for further discussion)

Figure 8 shows the equivalent electric circuit used to simulate the impedance spectrum of the aluminum surface without PPy film. In this model, R_1 represents the electrolyte solution resistance; C_1 and R_2 represent the capacitance and the resistance of the wall pores on the defective aluminum oxide layer; Q_1 and R_3 denote the double layer constant phase element and charge transfer resistance, and W is the Warburg impedance that measures the resistance of the electroactive species to move from the corroding surface to the bulk of the electrolyte, and vice versa. C_2 and R_4 represent the capacitance and resistance of the barrier oxide layer. The constant phase element Q can be interpreted as a deviation of the double layer from an ideal behaviour. This deviation is associated with surface roughness, porosity, mass transport or the presence of a defective oxide film [30–32]. The constant phase element Q is defined by

$$Z_q = (C(j\omega)^n)^{-1}$$

where C is the capacitance of an ideal capacitor. The number n, $0 < n < 1$, represents the deviation of the ideal capacitance behaviour ($n = 1$ represents an ideal capacitor), $j = (-1)^{-1/2}$ and ω is the angular frequency of the AC voltage applied in the electrolyte cell.

Figure 9 presents a comparison between the experimental results (empty circles and plus symbols) and the results of the simulation performed with the proposed equivalent electrical circuit (solid line). It indicates that the model may be used to

explain the behaviour of the aluminum surface exposed to the chloride medium. Table 2 shows the simulated parameter values.

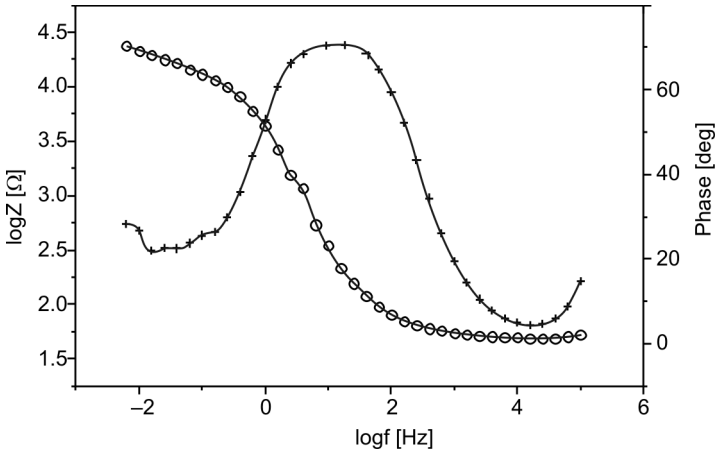

Fig. 9. Bode plot of the aluminum surface without PPy film. An equivalent electric circuit represented by $R_1(C_1[R_2(Q_1[R_3W])])$ (C_2R_4) in Boukamp notation was used to simulate the experimental results

Table 2. Electrochemical parameters obtained by simulation of the EIS results of the aluminum surfaces without PPy films and exposed to chloride medium

C_1	R_2	Q_1	n	$R_3 = R_{tc}$	W	C_2	R_4
2.2 pF	3.0 kΩ	$7.1 \cdot 10^{-2}$ μF	0.91	12.1 kΩ	2.77	31.1 μF	6.8 Ω

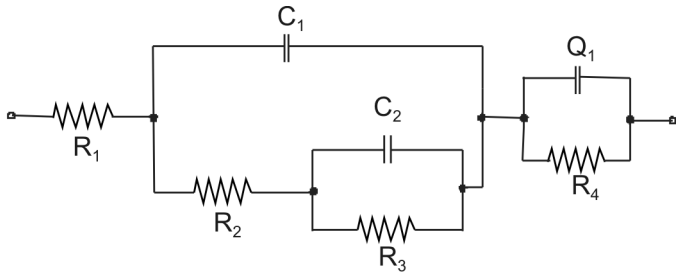

Fig. 10. Equivalent electric circuit model proposed to simulate the electrochemical behaviour of the aluminum surface coated with PPy films

The equivalent electric circuit shown in Fig. 10 was used to simulate the impedance spectra of the aluminum surface coated with the PPy films. In this model R_1 represents the electrolyte solution resistance; C_1 and R_2 represent the capacitance and the resistance of the pores wall of the polymer; C_2 and R_3 represent the capacitance and the resistance of the PPy film. Q_1 and R_4, respectively, denote the double layer

constant phase element and the charge transfer resistance in the interface metal/oxide, respectively.

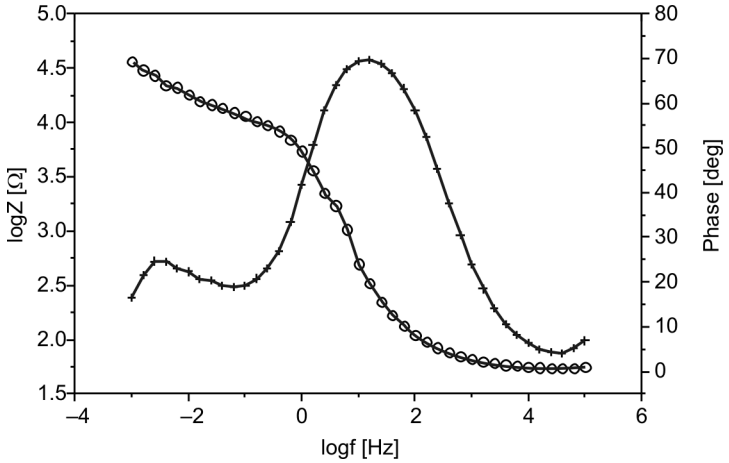

Fig. 11. Bode plot of the aluminum surface coated with PPy film deposited at 2.5 mA·cm^{-2}. An equivalent electric circuit represented by $R_1(C_1[R_2(C_2R_3)])$ (Q_1R_4) in Boukamp notation was used to simulate the experimental results

Figure 11 shows the comparison between experimental data (empty circles and plus symbols) and simulated (solid line) impedance results for aluminum surface coated with PPy film deposited at 2.5 mA·cm^{-2}. This result shows that the proposed model explains the behaviour of the aluminum surface coated with PPy films in chloride medium. Table 3 shows the values of simulated parameters for aluminum surfaces coated with PPy films electrodeposited at 2. 5 and 10 mA·cm^{-2}.

Table 3. Electrochemical parameters obtained by simulation of the EIS results of the aluminum surfaces coated with PPy films and exposed to chloride medium.

Electrochemical parameter	Aluminum surface coated with PPy deposited at 2.5 mA·cm^{-2}	Aluminum surface coated with PPy deposited at 10.0 mA·cm^{-2}
R_1 [Ω]	52.9	52.9
C_1 [μF]	16.7	10.5
R_2 [kΩ]	6.9	3.9
C_2 [mF]	3.9	9.6
R_3 [kΩ]	2.2	3.9
Q_1 [μF]	1.76	0.43
n	0.62	0.71
$R_4 = R_{tc}$ [kΩ]	13.6	1.09

The R_2 values attributed to resistance of PPy pores are higher for films deposited at 2.5 mA·cm^{-2} than for those formed at 10.0 mA·cm^{-2}. This parameter is associated with

defects along the polymeric chain. The smaller the R_2 value is, the higher is the number of defects on the coating.

The R_3 values attributed to the resistance into PPy are higher for the film deposited at 10.0 mA·cm^{-2} than for the film formed at 2.5 mA·cm^{-2}. A higher overoxidation degree for the films formed at 10 mA·cm^{-2} can explain the smaller contribution of reactions on the polymeric matrix. Furthermore, the capacitance of the polymer C_2 was smaller for the film deposited at 2.5 mA·cm^{-2} than for the film formed at 10.0 mA·cm^{-2}. The higher porosity of the latter films, as observed in the SEM micrographs in Fig. 4, explains the higher capacitance observed for this coating.

It was also observed that aluminum surfaces coated with PPy films deposited at 2.5 mA·cm^{-2} showed a smaller charge transfer resistance value R_4 than that observed for surfaces with PPy films deposited at 10.0 mA·cm^{-2}. The presence of larger voids in the film deposited at 10.0 mA·cm^{-2} (Fig. 4(c)) allows the penetration of aggressive ions (chloride) that assists the corrosion process.

Moreover, by comparing the charge transfer resistance values of the uncoated aluminum surfaces with those coated with PPy film, one can confirm the poor performance of PPy film studied in this work to protect aluminum surfaces against corrosion.

4. Conclusions

Films formed by the cyclic voltammetry are much less compact and uniform than those formed galvanostatically. Moreover, films formed at higher current densities are more susceptible to overoxidation than films formed at lower current densities, which was demonstrated by a much smaller microspherical grain size and bigger voids among the grains (SEM results) of PPy formed at higher current densities. This finding is also supported by the FTIR results, which demonstrated that the absorption bands at 1170 and 1630 cm^{-1} may be attributed to the overoxidation process of the PPy.

The polarization curves and impedance results showed that the PPy films presented in this work are not able to protect the aluminum surfaces against corrosion. It was observed that the corrosion current densities of the aluminum surfaces coated with PPy films were higher than those observed for uncoated surfaces. Furthermore, the aluminum surfaces coated with PPy film showed impedance values lower than those observed for the uncoated aluminum. Since higher values of impedance are associated with a higher resistance to corrosion, these results suggest that the coated surfaces present lower corrosion resistance than bare aluminum.

The overoxidation process results in pores and defects along the polymeric structure allowing the penetration of corrosive species and rendering the aluminium surfaces more susceptible to corrosion.

Acknowledgements

The authors thank the Fundação de Amparo à Pesquisa do Estado de São Paulo (FAPESP) for the financial support and the Alcoa Alumínio SA, São Luis, Maranhão, Brazil.

References

[1] INGRAM M.D., STAESCHE H., RYDER K.S., Solid State Ionics, 169 (2004), 51.
[2] AMEER Q., ADELOJU S.B., Sens. Actuators B., 106 (2005), 541.
[3] TALLMAN D.E., SOKINS G., DOMINIS A., WALLACE G.G., J. Solid State Electrochem., 6 (2002), 73.
[4] TRAMONTINA J., MACHADO G., AZAMBUJA D.S., PIANICKI C.M.S., SAMIOS D., Mater. Res., 4 (2001), 95.
[5] WENCHENG S., IROH J.O., Synth. Met., 95 (1998), 159.
[6] WANG L.X., LI X.G., YANG Y.L. React. Funct. Polymers, 47 (2001), 125.
[7] MALINAUSKAS A., Polymer, 42 (2001), 3957.
[8] AYAD M.M., Polym. Int., 35 (1994), 35.
[9] MARTINS N.C.T., MOURA T.S., MONTEMOR M.F., FERNANDES J.C.S., FERREIRA M.G.S., Electrochim. Acta 53 (2008), 4754.
[10] NAOI K., TAKEDA M., KANNO H., SAKAKURA M., SHIMADA A., Electrochim. Acta, 45 (2000), 3413.
[11] LEHR I.L., SAIDMAN S.B., Mater. Chem. Phys., 100 (2006), 262.
[12] BAZZAOUI M., MARTINS J.I., COSTA S.C., BAZZAOUI E.A., REIS T.C., MARTINS L., Electrochim. Acta, 51 (2006), 2417.
[13] SAIDMAN S.B, BESSONE J.B., J. Electroanal. Chem., 521 (2002), 87.
[14] SAIDMAN S.B., J. Electroanal. Chem., 534 (2002), 39.
[15] TSAI M.L., CHEN P.J., DO J.S., J. Power Sources, 133 (2004), 302.
[16] LIU A.S., OLIVEIRA M.A.S., J. Brazil. Chem. Soc., 18 (2007), 143.
[17] AKUNDY G.S., IROH J.O., Polymer, 42 (2001), 9665.
[18]. BRESLIN C.B., FENELON A.M., CONROY K.G., Mater. Des., 26 (2005), 233.
[19] ARENAS M.A., GONZALES BAJOS L., DAMBORENEA J.J., OCON P., Prog. Org. Coatings, 62 (2008), 79.
[20] HULSER P., BECK F., J. Appl. Electrochem., 20 (1990), 596.
[21] ASTM G 102-89, *Practice for Calculation of Corrosion Rates and Related Information from Electrochemical Measurements*, 1994.
[22] BOUKAMP B.A., Solid States Ionics, 1 (1986), 31.
[23] LI Y., QIAN R., Electrochim. Acta, 45 (2000), 1727.
[24] BAZZAOUI M., MARTINS L., BAZZAOUI E.A., MARTINS J.I., Electrochim. Acta, 47 (2002), 2953.
[25] MAZEIKIEN R., MALINAUSKAS A., Polym. Degrad. Stab., 75 (2002), 255.
[26] RODRIGUEZ I., SCHARIFKER B.R., MOSTANY J., J. Electroanal. Chem., 491 (2000), 117.
[27] BRUYNE A., DELPHANCKE J.L., WINAND R., Surface Coatings Techn., 99 (1998), 118.
[28] VILCA D.H., MORAES S.R., MOTHEO A.J., Synth. Met., 140 (2004), 23.
[29] OCON P., CRISTOBAL A.B., HERRASTI P., FATAS E., Corros. Sci., 47 (2005), 649.
[30] BISQUERT J., COMPTE A., J. Electroanal. Chem., 499 (2001), 112.
[31] PAJKOSSY T., KERNER Z., Electrochim. Acta, 46 (2000), 207.
[32] PAJKOSSY T., Solid State Ionics, 176 (2005), 1997.

Received 23 April 2008
Revised 19 December 2008